

## Synthesis and characterization of bacterial cellulose composite with graphite and TiO<sub>2</sub>-ZnO: structural and functional analysis

Muhammad Fariz Nafiir<sup>a</sup>, Sudirman<sup>a</sup>, Emmy Yuanita<sup>a</sup>, Sazmal E. Arshad<sup>b</sup>, Retno Ariadi Lusiana<sup>c</sup>, Maria Ulfa<sup>\*a</sup>

[a] Chemistry Department, Faculty of Mathematics and Natural Science, University of Mataram, Mataram-NTB, 83125 Indonesia

[b] Faculty of Science and Natural Resources, Universiti Malaysia Sabah, 88400 Kota Kinabalu, Sabah, Malaysia

[c] Department of Chemistry, Faculty of Science and Mathematics, Diponegoro University, 50275 Semarang, Indonesia. E-mail: [ulfaarief@unram.ac.id](mailto:ulfaarief@unram.ac.id)

DOI: 10.29303/aca.v7i2.204

### Article info:

Received 23/04/2024

Revised 20/06/2024

Accepted 27/08/2024

Available online 30/10/2024

**Abstract:** This research aims to synthesize and characterize a bacterial cellulose (BC)-based composite with graphite and TiO<sub>2</sub>-ZnO as reinforcement materials using ex-situ synthesis with CTAB as a surfactant. FTIR and SEM-EDS analysis revealed interactions between the matrix and the reinforcement materials, as well as irregular particle distribution in the BC/G-TiO<sub>2</sub>-ZnO composite. The addition of graphite to BC significantly increased the conductivity of the composite, while the addition of TiO<sub>2</sub>-ZnO had the opposite effect. The mechanical properties of the composite exhibited an inverse relationship with the conductivity parameter. Swelling tests indicated that pH and the addition of CTAB influenced the swelling behavior of the BC-based composite. The results of this study provide a strong foundation for the development of potential applications in the fields of electronics and pollutant filtration. The synthesis of this composite aims to harness the unique properties of BC, graphite, and TiO<sub>2</sub>-ZnO, creating a multifunctional material with potential uses in flexible electronics, sensors, biocompatible conductive materials, and advanced filtration systems.

**Keywords:** Bacterial Cellulose, Graphite, TiO<sub>2</sub>-ZnO, Composite, FTIR, SEM-EDS, Conductivity, Mechanical Properties, Swelling

**Citation:** Fariz Nafiir, M., Sudirman, Yuanita, E., Arshad, S. E., Lusiana, R. A., & Ulfa, M. (2024) Synthesis and characterization of bacterial cellulose composite with graphite and TiO<sub>2</sub>-ZnO: structural and functional analysis. *Acta Chimica Asiana*, 7(2), 478–486. <https://doi.org/10.29303/aca.v7i2.204>

### INTRODUCTION

In recent decades, scientists have focused on the research and development of composite materials in various scientific fields, including materials engineering, nanotechnology, and electronics such as capacitors [1], and battery separators [2], as well as biotechnology [3]. Composite materials offer unique properties and performance that cannot be achieved by single materials alone, due to the synergy between the matrix and reinforcement materials. The composite matrix acts as a binding material that withstands and distributes the forces acting on the composite, while the reinforcement materials provide additional strength and special properties. To achieve this, scientists have combined different types

of materials to create new composites with improved properties that can be used for specific purposes.

Composites consist of a matrix or binder material and a filler or reinforcement material. In recent years, bacterial cellulose (BC), which is a natural polymer produced by bacteria, has garnered attention as a binder material. BC is mainly produced by bacteria from the *Acetobacter* and *Gluconacetobacter* genera through the fermentation of glucose or other carbohydrates. It has many advantages due to its unique properties and natural nanofibril structure that easily binds with fillers [4], resulting in exceptional mechanical properties, good dimensional stability, and high biodegradability. Additionally, it has unique

surface properties that enable strong adhesion with various fillers and matrices [5]. Meanwhile, graphite (G) and TiO<sub>2</sub>-ZnO are two types of fillers commonly used in composite synthesis. Graphite, made of carbon with a layered crystal structure, exhibits high thermal and electrical conductivity and good adsorption properties towards organic pollutants. On the other hand, TiO<sub>2</sub>-ZnO is a semiconductor material with numerous potential applications in photocatalysis and electronics. Previous studies have successfully synthesized and characterized polysaccharide-based hybrids with graphene, carbon nanotubes, and metal oxide as fillers [6]. These composites are a promising solution for effective pollutant filtration. According to Bodzek et al. (2020), these fillers provide the composite with good adsorption properties towards organic pollutants and photocatalytic properties that can break down pollutants into simpler and harmless compounds [7]. The sustainability of using these composites is also considered due to their biodegradability. The metal oxides and graphene can improve BC's crystallinity and pollutant filtration effectiveness in composite membranes [6].

Metal oxide fillers are known to enhance the physical and mechanical properties of BC. One such filler is TiO<sub>2</sub> and ZnO, which have been commonly used in research [8]. TiO<sub>2</sub> and ZnO have individual positive effects on the properties of BC. TiO<sub>2</sub> improves thermal balance and mechanical properties, has a high surface area, and improves fire resistance [9]. On the other hand, ZnO enhances the stability of physical and chemical properties, exhibits photocatalytic activity, functions as a natural semiconductor, provides good electron carrier mobility, and has high absorbance capacity [10]. The combination of these two metal oxides is expected to have an even greater positive impact [11].

The BC/G composite has been successfully synthesized ex-situ by incorporating CTAB (Cetyltrimethylammonium bromide), as demonstrated in the research conducted by [12]. Furthermore, the addition of a TiO<sub>2</sub>-ZnO mixture to the BC/G composite was carried out with modifications based on the studies by [13] and [8] for the fabrication of BC/G-TiO<sub>2</sub>-ZnO composites. Subsequently, the composites underwent characterization to determine their morphology, physical and chemical properties, as well as mechanical properties. This research is expected to make a positive contribution to the development of potential applications for BC-based composites in flexible electronics, sensors, biocompatible

conductive materials, and advanced filtration systems.

## MATERIALS AND METHODS

### Materials

The materials used in this study included bacterial cellulose pellicles obtained from UMKM NATA Yogyakarta. The bacterial cellulose pellicle was produced using *G. xylinus* and coconut water as the medium. Other materials used were H<sub>2</sub>O, ethanol (Merck), n-butanol 80% v/v (Sigma-Aldrich), Cetyl trimethylammonium bromide (CTAB) (Merck), graphite (Merck), TiO<sub>2</sub> (Merck), ZnO (Merck), NaOH (Merck), and buffer solutions with pH values of 1.2, 4.5, 6.4, 6.86, 7.4, and 8.4 (Sigma-Aldrich).

### Fabrication of BC/G and BC/G-TiO<sub>2</sub> Composites

The BC/G composite was created by following the method described by [11], with some modifications. First, a solution of graphite (0.5% (w/v)) was prepared by dissolving 5 g of calcined graphite (1000 °C, 5 minutes) in water (100 mL) and adding CTAB (0.3% (w/v)), followed by 7 hours of sonication. Next, a piece of bacteria cellulose (measuring 8 cm x 8 cm), with known water content and weight, was placed in the graphite solution (0.5% (w/v)) and homogenized by sonication for 6 hours at 25 °C. The resulting BC/G composite was weighed, pressed, and dried for two days at room temperature to obtain the final BC/G composite.

The BC/G-TiO<sub>2</sub>-ZnO composite was prepared using a similar method as described in the studies by [12] and [8], with some modifications. To obtain the G-TiO<sub>2</sub>-ZnO solution (2:1:1), a graphite solution (0.5% (w/v), 50 mL) was mixed with TiO<sub>2</sub>-ZnO solution (1:1, 50 mL). The bacterial cellulose (measuring 8 cm x 8 cm) was then immersed in the G-TiO<sub>2</sub>-ZnO solution (2:1:1) and homogenized by sonication for 3 hours at 25 °C. The resulting composite was weighed, pressed, and dried for two days at room temperature to obtain the BC/G-TiO<sub>2</sub>-ZnO composite.

### Characterization

SEM-EDS was used to conduct morphological and weight fraction studies of the composite components at the Integrated Laboratory of Mataram State Islamic University, Indonesia. The composite film was cut into 10 mm x 10

mm and coated with a 10 nm gold layer before being observed at magnifications ranging from 500-10,000x.

To analyze the functional groups, FTIR analysis was carried out. The composite film was cut into 10 mm x 10 mm and scanned in the wavenumber range of 4000 to 500  $\text{cm}^{-1}$  with a resolution of 4  $\text{cm}^{-1}$ . The analysis was conducted using Spectrum One, PerkinElmer located at the Integrated Laboratory of Mataram State Islamic University, Indonesia.

Thickness testing was measured using a digital screw micrometer thickness gauge (Mitutoya 547-321). Thickness measurements were taken at ten different points in the sample area. The thickness can be calculated using equation (1),  $\bar{t}$  represents the average thickness (mm),  $n$  is the number of data points, and  $t_n$  represents the thickness (mm).

$$\bar{t} = \frac{t_1 + t_2 + \dots + t_n}{n} \quad (1)$$

Mechanical testing or tensile strength was performed using a Tensilon RTG-1310 instrument with a 5.0 kN load cell capacity and a 5 mm/min sample withdrawal speed. The tensile strength and sample length at fracture were determined from the average values obtained based on equation (2).  $\sigma_t$  represents the tensile strength ( $\text{N/cm}^2$ ),  $F_t$  represent the tensile force perpendicular to the surface (N), and  $A_t$  represents the cross-sectional area of the specimen being pulled ( $\text{cm}^2$ ).

$$\sigma_t = \frac{F_t}{A_t} \quad (2)$$

Porosity testing was conducted by measuring the sample's dry and wet weight after soaking it in 80% n-butanol solution at room temperature for 1 hour. The testing was repeated three times. The percentage of sample porosity was calculated using equation (3). The porosity (%), represented by  $\phi$ , can be calculated using the following variables: the dry mass of the sample ( $M_k$ ) in grams, the wet mass of the sample ( $M_b$ ) in grams, the density of n-butanol ( $\rho_B$ ) in grams per cubic centimeter, the volume of the dry sample ( $V_k$ ) in cubic centimeters, and the sample radius ( $r$ ) in centimeters.

$$\phi = \frac{(M_b - M_k)}{\rho_B \times V_k} \times 100 \% \quad (3)$$

where,

$$V_k = \pi \times r^2 \times t$$

Electrolyte testing was performed by measuring the sample's dry and wet weight after soaking it in a 1M NaOH solution at room temperature for 1 hour. The testing was

repeated three times. The percentage of electrolyte absorption was determined using equation (4).  $A_e$  represents the electrolyte absorption (%).

$$A_e = \frac{(M_b - M_k)}{M_k} \times 100 \% \quad (4)$$

Conductivity testing was carried out using a conductivity meter by passing an electric current through the sample. The measurement of conductivity can be obtained using equation (5). In the equation,  $k$  represents the electrical conductivity (S/m),  $R$  represents the resistance ( $\Omega$ ),  $V$  represents the voltage (V),  $I$  represents electrical current (A),  $\rho$  represents the resistivity ( $\Omega\text{cm}$ ), and  $l$  represents the length of the sample (cm).

$$k = \frac{1}{\rho} \quad (5)$$

where,  $\rho = \frac{R \times A}{l}$ ;  $R = \frac{V}{I}$ ;  $A = \frac{l}{t}$

The mechanical characteristics of the composite materials were evaluated using a Tensilon RTG-1310 tensile strength testing apparatus. Tensile specimens of the composites were prepared following coupon type specifications (JIS K7113), with dimensions of 115 mm x 25 mm x 1 mm. Tensile tests were conducted on the BC composite specimens at a temperature of 298 K (25°C) and a relative humidity of 55%. The specimens were subjected to uniaxial tension along the longitudinal direction, and the relationship between the applied load ( $P$ ) and the corresponding displacement ( $\delta$ ) at the loading point was recorded. The testing speed was maintained at a constant rate of 0.2 mm/min throughout the tests.

Swelling testing was determined by calculating the sample's dry and wet weight after immersing it in different pH solutions at room temperature for 30-minute intervals for 4.5 hours. The testing was repeated three times. The percentage of swelling was determined using equation (6).  $W_s$  represents the wet sample mass (g), and  $W_d$  represents the dry sample mass (g).

$$WAC = \frac{(W_s - W_d)}{W_d} \times 100 \% \quad (6)$$

## RESULTS AND DISCUSSION

### Morphology

According to the SEM analysis shown in Figure 1, there is an interaction between BC as the matrix and graphite,  $\text{TiO}_2\text{-ZnO}$  as fillers. When graphite is added to the bacterial cellulose composite, as seen in Figure 1A, the

graphite particles are evenly dispersed as flakes within the bacterial cellulose matrix. This creates a hybrid structure where the graphite flakes are intercalated between the cellulose fibers. The addition of the surfactant CTAB reduces the crystal size in BC and creates more pores, allowing more graphite to enter the BC pores more easily [14]. As a result, this composite has increased electrical conductivity due to the synergistic effect of bacterial cellulose and graphite. This morphology provides advantages in flexible electronics,

sensors, and biocompatible conductive materials.

Regarding the toxicity of the composite, further tests are necessary to evaluate the biocompatibility and environmental safety of the BC/G-TiO<sub>2</sub>-ZnO composite. Preliminary studies suggest that while BC and graphite are biocompatible, the incorporation of TiO<sub>2</sub>-ZnO may introduce potential cytotoxicity. Therefore, it is crucial to conduct thorough toxicity assessments to ensure the safe application of these composites in real-world scenarios.

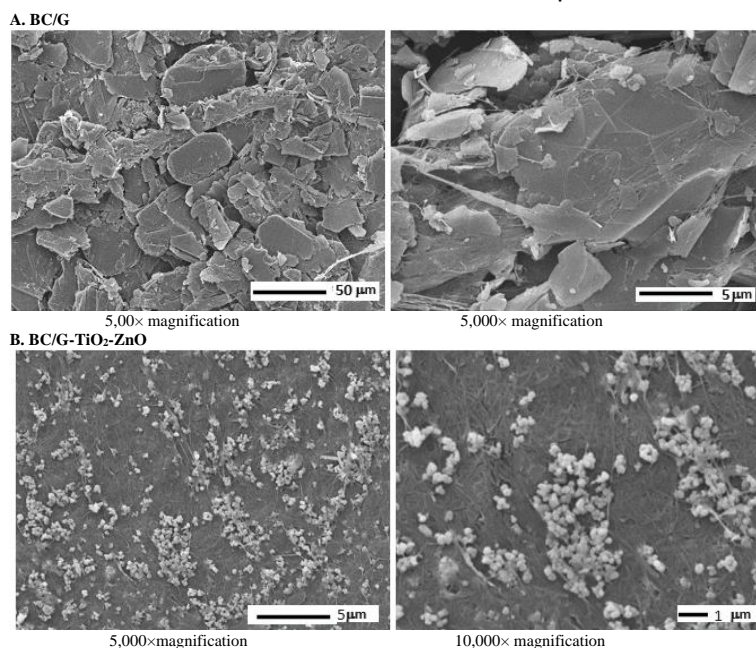


**Figure 1.** SEM images of dried (A) BC/G and (B) BC/G-TiO<sub>2</sub>-ZnO composites

**Table 1.** EDS analysis for composites

Composites	Mass (%)			
	C	O	Ti	Zn
BC	32.94±0.33	67.06±0.87	-	-
BC/G	57.38±0.42	42.62±0.95	-	-
BC/G-TiO <sub>2</sub> -ZnO	27.68±0.31	66.96±0.88	4.34±0.23	1.02±0.31

The BC/G-TiO<sub>2</sub>-ZnO composite (as shown in Fig. 1B) consists of graphite, TiO<sub>2</sub>, and ZnO particles that are dispersed irregularly within the matrix. These particles tend to cluster around the edges of the fibers and form thin layers along the fiber surface, although there are also some areas where the particles appear to be agglomerated. Upon closer inspection, it is observed that the surfaces of these particles are rough and irregular, which is likely due to agglomeration or aggregation during the composite's synthesis or drying process. Despite this, the composite structure shows promise for use in catalysis and photocatalysis. However, it may be necessary

to improve particle dispersion to enhance the overall reaction efficiency and composite properties.

An EDS analysis was conducted on the BC/G composite, and the results are presented in Table 1. The analysis revealed that the composite contains graphite within the BC matrix, which is indicated by a nearly twofold increase in the amount of carbon (C) element when compared to the BC composite. Furthermore, the analysis also detected the presence of titanium (Ti) and zinc (Zn) in the BC/G composite. These elements constitute approximately 1-4% of the total composite mass. The presence of Ti and Zn in the

composite causes a decrease in the percentage mass of C. This indicates that the addition of TiO<sub>2</sub> and ZnO affects the overall composition of the BC/G matrix, thereby altering the relative amounts of various existing elements.

### FTIR Analysis

Fig. 2 illustrates the composition and interactions among BC material with graphite filler and the TiO<sub>2</sub>-ZnO metal mixture, as seen from the FTIR spectra. All three composites exhibit characteristic peaks related to the cellulose structure, such as broad O-H stretching, C-H stretching, C-O-C stretching, and C-O stretching. The FTIR spectrum of BC demonstrates characteristic peaks associated with cellulose, including O-H stretching vibrations between 3300-3500 cm<sup>-1</sup> [15], C-H stretching vibrations in the range of 2900-3000 cm<sup>-1</sup> [16], C-O-C stretching vibrations around 1100-1165 cm<sup>-1</sup>, and C-O stretching vibration around 1000-1050 cm<sup>-1</sup>. Additionally, bending vibrations of the hydroxyl group are observed at peaks around 1600-1640 cm<sup>-1</sup> and 1420-1430 cm<sup>-1</sup>, while glycosidic linkages within the cellulose backbone manifest as a prominent peak at approximately 900-1100 cm<sup>-1</sup> [17][18].

The presence of graphite in bacterial cellulose creates additional peaks associated with its structure, such as a prominent G-band peak around 1570-1700 cm<sup>-1</sup> and a less intense D-band peak around 1300-1400 cm<sup>-1</sup>. These peaks characterize the sp<sup>2</sup> carbon atoms in graphite and were confirmed in the FTIR spectrum, along with cellulose peaks, which confirm the successful incorporation of graphite into the bacterial cellulose matrix [18]. Moreover, new peaks may appear when TiO<sub>2</sub> and ZnO nanoparticles are added to the bacterial cellulose/graphite composite. These peaks, which are related to Ti-O stretching vibrations (usually between 500-700 cm<sup>-1</sup> for TiO<sub>2</sub>) and Zn-O stretching vibrations (around 400-500 cm<sup>-1</sup> for ZnO), indicate the successful incorporation of these nanoparticles into the composite structure [19].

### Physical Properties

The physical properties of BC-based composites can be significantly impacted by the addition of graphite and G-TiO<sub>2</sub>-ZnO fillers, as shown in Table 2. The conductivity of BC/G is 300 times higher than that of BC alone due to the incorporation of graphite and the

cationic surfactant CTAB into the BC matrix. Intercalation of graphite into the BC matrix can be induced by adding CTAB to graphite. This intercalation can enhance conductivity by providing additional conductive paths for electrical current between graphite layers and BC fibers, resulting in an increased composite thickness. However, intercalation can also affect the pore structure of the composite material as graphite can quickly enter the pores of the BC matrix.

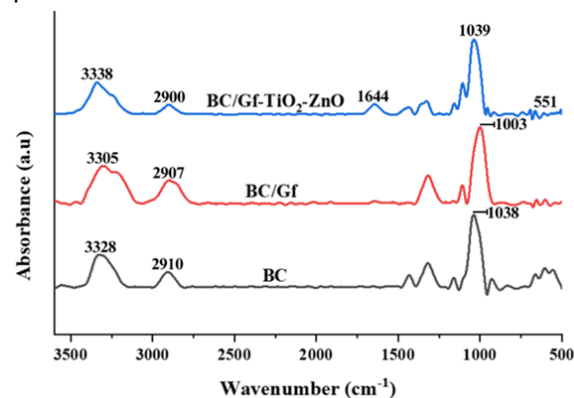


**Figure 2.** FTIR Spectra of BC, BC/G, and BC/G-TiO<sub>2</sub>-ZnO composites

It has been observed that the addition of TiO<sub>2</sub>-ZnO filler to the BC/G matrix can disrupt the intercalation process due to changes in the chemical properties of the filler, including its size, structure, acidity, or alkalinity. It has also been noted that the decrease in thickness is likely caused by the TiO<sub>2</sub>-ZnO particles filling more space in the matrix, leading to a denser and stiffer composite. According to Wahid et al. (2022), the addition of TiO<sub>2</sub>-ZnO can increase porosity [8]. These metal oxides are nanoparticle-sized, which means they can disperse efficiently and form nano-sized pores. However, the agglomeration of G-TiO<sub>2</sub>-ZnO particles on the surface of the BC matrix (as shown in Fig. 1B) can disrupt the homogeneous distribution of electrolytes in the composite, leading to a reduction in the composite's ability to conduct electrolytes. This results in decreased conductivity of the composite due to hindered movement of electric charges. Therefore, it is crucial to overcome particle agglomeration in composite synthesis to maintain optimal electrochemical properties and conductivity in further research by varying the concentration and type of surfactant.

Table 2. Physical Properties of Composites based on BC

Composites	Thickness ( $\mu\text{m}$ )	Porosity (%)	Electrolyte (%)	Conductivity ( $\times 10^{-2}$ S/m)
BC	43.7 $\pm$ 0.2418	48.0 $\pm$ 9.5969	171.4 $\pm$ 60.093	1.87
BC/G	79.0 $\pm$ 0.2371	26.5 $\pm$ 2.2543	321.4 $\pm$ 23.154	335.44
BC/G-TiO <sub>2</sub> -ZnO	64.6 $\pm$ 0.3658	29.2 $\pm$ 5.6223	180.0 $\pm$ 41.944	0.48

### Mechanical Properties

According to Susilo et al. (2021), the addition of graphite as a filler in bacterial cellulose-based composites can improve their mechanical properties [14]. The presence of CTAB as a surfactant poses challenges to the mechanical properties of the composite. This is because CTAB can affect the hydrogen bonding within the composite network or lead to changes in interactions within the composite matrix, ultimately reducing its mechanical strength. Moreover, the presence of CTAB can cause the agglomeration of composite fillers, which affects the adhesion between molecules in the matrix and further reduces its mechanical strength. Therefore, while CTAB is beneficial for dispersing the fillers, its concentration needs to be optimized to balance the mechanical properties and other functional attributes of the composite.

It has been found that adding TiO<sub>2</sub>-ZnO to BC/G composites has a significant impact on the mechanical properties and Young's modulus of the composite. Graphite provides additional structural reinforcement to the BC matrix, while TiO<sub>2</sub>-ZnO enhances the tensile strength and stiffness of the composite by providing a solid interfacial interaction between the polymer matrix and the filler [20][21][22]. Moreover, the TiO<sub>2</sub>-ZnO composite helps to prevent filler agglomeration within the matrix, thereby improving the homogeneous distribution of fillers and reducing structural defects. As a result, the Young's modulus of the composite increases due to the formation of stronger bonds between composite phases.

### Swelling Behavior

Results of swelling tests conducted to study the time-dependent swelling behavior of BC, BC/G, and BC/G-TiO<sub>2</sub>-ZnO are summarized in Figures 4 and 5. The surface of BC contains numerous hydroxyl groups (-OH) that promote hydrogen bonding. This property contributes to good composite formation, high water retention, and fast swelling rates. However, when other components are added to the BC matrix, the hydrogen bonding on the BC surface is disrupted, leading to changes in the swelling behavior of BC-based composites [23]. Additionally, changes in pH in acidic and

alkaline media can also affect the surface charge of BC due to the influence of hydrogen ions (H<sup>+</sup>) and hydroxide ions (OH<sup>-</sup>) in the media on the functional groups of the BC surface. The surface charge will influence the electrostatic interactions between the components within the BC matrix and the surrounding environment [24].

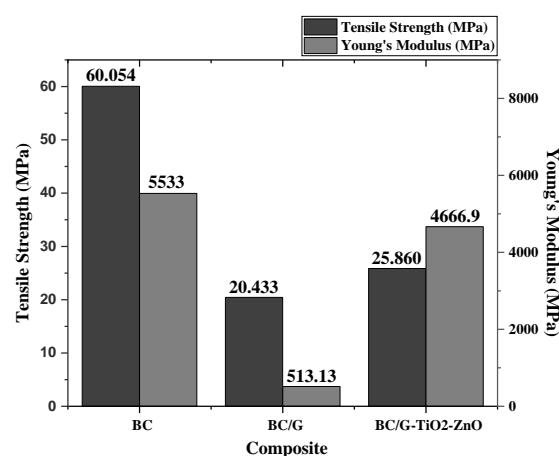


Figure 3. Tensile strength and Young's modulus of BC-based composite

When the pH of the environment is high (alkaline), the surface of BC usually becomes negatively charged because of the deprotonation of hydroxyl groups (-OH). This makes BC more hydrophilic and causes it to swell more than in a low pH environment (as shown in Fig. 4 and 5B). The addition of graphite and CTAB surfactant to the BC matrix creates electrostatic, hydrophobic, and cation- $\pi$  electron interactions that can affect the swelling performance. As shown in Fig. 4 and 5A, the BC/G composite has the lowest swelling percentage at pH 1.2. This is because the surface of BC tends to be positively charged due to the protonation of hydroxyl groups (-OH). The electrostatic interaction between the positively charged BC and the positively charged quaternary ammonium head group on CTAB can be strengthened, which enhances the absorption of CTAB on the BC surface [25]. This also improves the interaction between CTAB and graphite, increasing the hydrophobic interaction between the alkyl tail of CTAB and the BC and graphite surfaces.

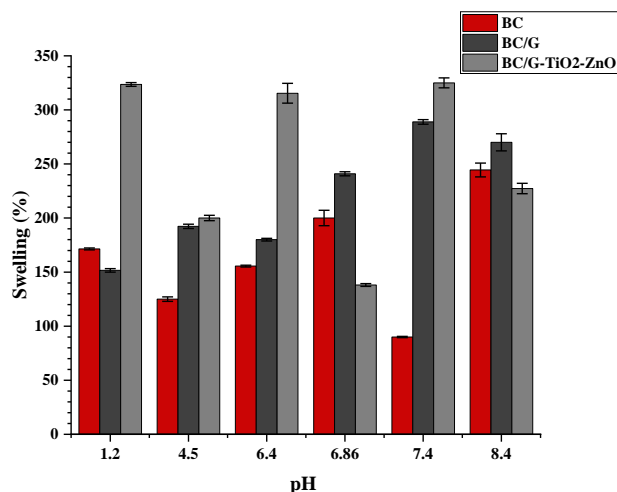


Figure 4. Effect of pH on the swelling percentage of composite-based BC

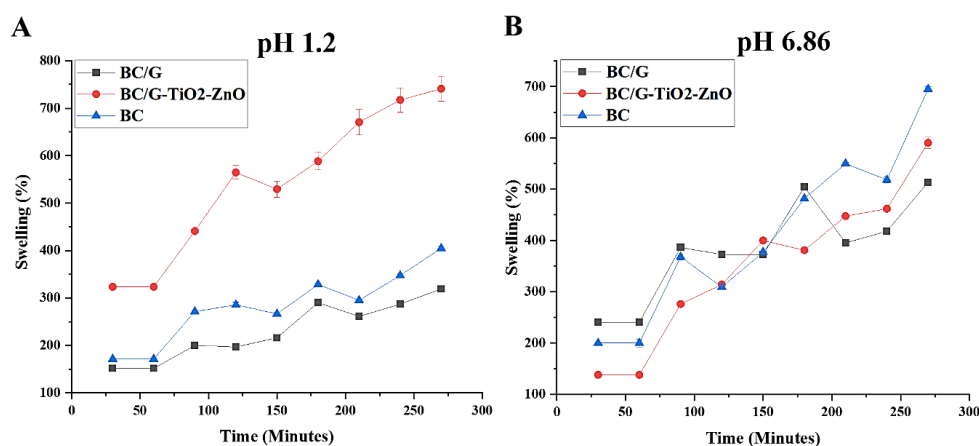


Figure 5. Effect of time swelling percentage of the composites at pH A. 1.2 and B. 6.86.

The addition of a mixture of TiO<sub>2</sub>-ZnO significantly increases the swelling of the composite, particularly at pH 1.2, in comparison to BC and BC/G composites (as shown in Fig. 4 and 5A). At low pH, the surface of graphite undergoes protonation and becomes more hydrophilic. TiO<sub>2</sub>-ZnO is amphoteric, and in an acidic environment, hydrogen ions interact with the hydroxyl groups on its surface, forming ion bonds that increase swelling. CTAB assists in dispersing and adhering these fillers into the BC matrix, reducing the surface tension of water, allowing water to penetrate the composite, and enhancing swelling.

The influence of time and pH (1.2 and 6.86) on the percentage of swelling of the composites can be seen in Figure 5. At low pH (1.2), the swelling percentage of the composites increases significantly over time, and the composites do not show degradation until 270 minutes (Fig 5A). The BC/G-TiO<sub>2</sub>-ZnO

composite has the highest swelling percentage at pH 1.2, which is 2.14 times (30 minutes) and 2.9 times (270 minutes) compared to the BC/G composite due to the reasons mentioned earlier. At pH 6.86, BC/G shows the highest swelling percentage at 30 minutes compared to the other two composites, but after 180 minutes, the swelling percentage does not experience a significant increase. In an alkaline environment, the surface of BC/G undergoes deprotonation, which can reduce the bonding strength between BC and graphite as well as between BC and CTAB. Additionally, it can also affect the structure of the BC matrix, resulting in changes in morphology and mechanical properties or degradation over time.

## CONCLUSION

This study clarifies the importance of developing bacterial cellulose (BC)-based composites reinforced with graphite and a

TiO<sub>2</sub>-ZnO metal mixture. SEM and FTIR analyses revealed interactions among the composite components while swelling tests demonstrated the BC surface's sensitive response to environmental changes. Although the addition of graphite enhances the composite conductivity, the presence of CTAB as a surfactant poses challenges to the mechanical properties. However, the incorporation of graphite and TiO<sub>2</sub>-ZnO strengthens the composite structure and enhances interfacial interactions. Nonetheless, the challenges lie in managing particle distribution and optimizing the synthesis process. This research provides valuable insights into the potential and challenges in developing BC composites for future applications, such as in the fields of flexible electronics, due to the enhanced conductivity provided by graphite, and pollutant filtration, leveraging the photocatalytic properties of TiO<sub>2</sub>-ZnO. Managing particle distribution and optimizing the synthesis process is critical for improving the composite's performance and expanding its application range.

## REFERENCES

- [1] Blomquist, N., Engstrom, A. C., Hummelgard, M., Andres, B., Forsberg, S., & Olin, H. (2016). Large-Scale Production of Nanographite by Tube-Shear Exfoliation in Water. *Plos One*, 11(1), 1-11.
- [2] Ulfa, M., Noviani, I., Yuanita, E., Dharmayani, N. K. T., Sudirman, & Sarkono. (2023). Synthesis and Characterization of Composites-Based Bacterial Cellulose by Ex-Situ Method as Separator Battery. *Jurnal Penelitian Pendidikan IPA*, 9(6), 4647-4651.
- [3] Choi, S. M., Rao, K. M., Zo, S. M., Shin, E. J., & Han, S. S. (2022). Bacterial Cellulose and Its Applications. *Polymers*, 14(1080), 1-44.
- [4] Zhong, C. (2020). Industrial-Scale Production and Applications of Bacterial Cellulose. *Frontiers in Bioengineering and Biotechnology*, 8(605374), 1-19.
- [5] Gregory, D. A., Tripathi, L., Fricker, A. T., Asare, E., Orlando, I., Raghavendran, V., & Roy, I. (2021). Bacterial cellulose: A smart biomaterial with diverse applications. *Materials Science and Engineering: R: Reports*, 145, 100623.
- [6] Vilela, C., Pinto, R. J. B., Pinto, S., Marques, P., Silvestre, A., & Barros, C. S. D. R. F. (2018). Polysaccharide-based hybrid materials: metals and metal oxides, graphene, and carbon nanotubes. Springer.
- [7] Bodzek, M., Konieczny, K., & Kwiecińska-Mydlak, A. (2020). The application of nanomaterial adsorbents for the removal of impurities from water and wastewaters: a review. *Desalination and Water Treatment*, 185, 1-26.
- [8] Wahid, F., Zhao, X. Q., Cui, J. X., Wang, Y. Y., Wang, F. P., Jia, S. R., & Zhong, C. (2022). Fabrication of Bacterial Cellulose with TiO<sub>2</sub>-ZnO Nanocomposites as a Multifunctional Membrane for Water Remediation. *Journal of Colloid and Interface Science*, 620(1), 1-13.
- [9] Jayanthi, S., Shenbagavalli, S., Muthuvinnayagam, M., & Sundaresan, B. (2022). Effect of Nano TiO<sub>2</sub> on The Transport, Structural and Thermal Properties of PEMA-Nal solid polymer electrolytes for Energy storage devices. *Material Science Engineering: B*, 285, 115942.
- [10] Ul-Islam, M., Khattak, W. A., Ullah, M. W., Khan, S., & Park, J. K. (2014) Synthesis of Regenerated Bacterial Cellulose-Zinc Oxide Nanocomposite Films for Biomedical Applications. *Cellulose*, 21(1), 433-447.
- [11] Ramadhika, L. N., Aprilia, A., & Safriani, L. (2021). Studi Preparasi Senyawa ZnO: TiO<sub>2</sub> Sebagai Material Fotokatalis. *Jurnal Material dan Energi Indonesia*, 11(2), 83-95.
- [12] Aritonang, H. F., Wulandari, R., & Wuntu, A. D. (2020). Synthesis and Characterization of Bacterial Cellulose/Nano-Graphite Nanocomposite Membranes. *Macromolecular Symposia*, 391(1900145), 1-7.
- [13] Al-arjan, W. S., Khan, M. U. A., Almutairi, H. H., Alharbi, S. M., & Razak, S. I. A. (2022). pH-Responsive PVA/BC-f-GO Dressing Material for Burn and Chronic Wound Healing with Curcumin Release Kinetics. *Polymers*, 14(1949), 1-16.
- [14] Susilo, B. D., Suryanto, H., & Aminuddin. (2021) Characterization of Bacterial Nanocellulose–Graphite Nanoplatelets Composite Films. *Journal of Mechanical Engineering Science and Technology*, 5(2), 145-154.
- [15] Feng, Y., Zhang, X., Shen, Y., Yoshino, K., & Feng, W. (2012). A mechanically strong, flexible, conductive film based on bacterial cellulose/graphene nanocomposite. *Carbohydrate polymers*, 87(1), 644-649.



- [16] Zhu, C., Li, F., Zhou, X., Lin, L., & Zhang, T. (2014). Kombucha-synthesized bacterial cellulose: Preparation, characterization, and biocompatibility evaluation. *Journal of Biomedical Materials Research Part A*, 102(5), 1548-1557.
- [17] Czaja, W., Romanovicz, D., & Brown Jr, R. M. (2004). Structural investigations of microbial cellulose produced in stationary and agitated culture. *Cellulose*, 11(4), 403-411.
- [18] Ybañez, M. G., & Camacho, D. H. (2021). Designing hydrophobic bacterial cellulose film composites assisted by sound waves. *RSC advances*, 11(52), 32873-32883.
- [19] Mubari, P. K., Beguerie, T., Monthieux, M., Weiss-Hortala, E., Nzihou, A., & Puech, P. (2022). The X-ray, Raman, and TEM signatures of cellulose-derived carbons explained. *C*, 8(1), 4.
- [20] Annu, Bhat, Z. I., Imtiyaz, K., Rizvi, M. M. A., Ikram, S., & Shin, D. K. (2023). Comparative Study of ZnO-and-TiO<sub>2</sub>-Nanoparticles-Functionalized Polyvinyl Alcohol/Chitosan Bionanocomposites for Multifunctional Biomedical Applications. *Polymers*, 15(16), 3477.
- [21] Ali, H. A., & Hameed, N. J. (2022). Preparation of cellulose acetate nanocomposite films based on TiO<sub>2</sub>-ZnO nanoparticles modification as food packaging applications. *Journal of Applied Sciences and Nanotechnology*, 2(3), 115-125.
- [22] Cazan, C., Enesca, A., & Andronic, L. (2021). Synergic effect of TiO<sub>2</sub> filler on the mechanical properties of polymer nanocomposites. *Polymers*, 13(12), 2017.
- [23] Zhang, L., Yu, Y., Zheng, S., Zhong, L., & Xue, J. (2021). Preparation and properties of conductive bacterial cellulose-based graphene oxide-silver nanoparticles antibacterial dressing. *Carbohydrate Polymers*, 257, 117671.
- [24] Aditya, T., Allain, J. P., Jaramillo, C., & Restrepo, A. M. (2022). Surface modification of bacterial cellulose for biomedical applications. *International journal of molecular sciences*, 23(2), 610.
- [25] Ameh, T., Zarzosa, K., Dickinson, J., Braswell, W. E., & Sayes, C. M. (2023). Nanoparticle surface stabilizing agents influence antibacterial action. *Frontiers in Microbiology*, 14, 1119550.